Progress In Electromagnetics Research M, Vol. 94, 201–208, 2020

A Contactless System for the Dielectric Characterization of Liquid Drops

Gabriel Galindo-Romera[1], Javier Carnerero-Cano[2], José J. Martínez-Martínez[3], Alejandro Rivera-Lavado[3, 4], and Francisco J. Herraiz-Martínez[5, *]

Abstract—The present article shows the design, implementation, and measurement of a compact contactless electronic system for sensing small volumes of liquids. The system is based on two elements: an electronic reader and a passive sensor. The proposed sensor consists of a printed monopole antenna loaded with two Split-Ring Resonators. This results in a fully-passive and single-layer low-cost design. To allow the sensing of small volumes of liquids, a 1-mm-thick adhesive Kapton layer was attached on the top layer of the sensor, and two drop tanks were added to the structure. On the other hand, the reader was designed following a layered approach, which allows us to develop compact and low-cost electronic sensor readers for the Internet of Things. The resulting reader contains a Radio-Frequency interface for the generation of detection of signals, a minicomputer, and the radiating interface. This interface includes a patch antenna that allows us to interrogate the contactless sensor within a 1-cm range. The whole system was manufactured and tested. The total dimensions of the reader are 15 cm $\times$ 15 cm, and its weight is below 1 kg. These imply a dramatic form factor and weight reductions with respect to previous readers. Moreover, the manufactured system was used to measure the dielectric permittivity of different liquid drops. Results show that only 4 ml of liquid were needed to determine the dielectric permittivity with a 0.27% error. This volume means a 98.4% reduction compared to submersible sensors which can be found in the literature.

1. INTRODUCTION

Over the last few years, a wide variety of passive radio frequency (RF) sensors have been reported in the literature [1–6]. These sensors have been proposed for a wide variety of applications, such as agriculture [1], medicine [2, 3], or corrosion characterization [4]. Recently, the authors proposed different sensors based on Split-Ring Resonators (SRRs) for the characterization of the dielectric permittivity of solid and liquid materials [7, 8]. SRRs have been used in different applications such as sensors [7, 8] and antennas [9–11]. These resonators are very useful for the proposed application due to their small dimensions and high quality factor, which make them very compact and sensitive. In particular, the authors presented a submersible sensor for high volumes of liquids in [7]. Moreover, a contactless sensor for the dielectric characterization of solid materials was proposed in [8]. However, there is a demand for the characterization of small volumes of liquid samples in bioengineering applications. For example, some recent works propose the use of sensors for the measurement of glucose concentrations in liquids [12, 13]. Other works are focused on the dielectric characterization of oils [14, 15], which is really important in chemical and food industries. In this paper, we will tackle this last application.

Received 14 May 2020, Accepted 22 July 2020, Scheduled 1 August 2020

* Corresponding author: Francisco Javier Herraiz-Martínez (fjherraiz@icai.comillas.edu).

[1] Indra, Torrejón de Ardoz, Madrid, Spain. [2] Department of Computing, Imperial College London, London, United Kingdom. [3] Departamento de Teoría de la Señal y Comunicaciones, Universidad Carlos III de Madrid, Leganés, Madrid, Spain. [4] Yebes Observatory, Spanish National Geographic Institute, Yebes, Spain. [5] Instituto de Investigación Tecnológica (IIT), Escuela Técnica Superior de Ingeniería ICAI, Universidad Pontificia Comillas, Madrid, Spain.

Nowadays, most of the passive RF sensors are measured with laboratory instruments. This fact dramatically increases the total cost of the system and obliges the operation by qualified personnel. On the other hand, there are some proposals which present a full wireless solution but without including capabilities for the Internet of Things (IoT) [5, 6]. For all these reasons, the authors proposed, in [16], a full IoT system working wirelessly within a 11 cm range approximately. However, the main disadvantage of that proposal is that the sensor and reader had no integrated antennas which increased the form factor of the system, resulting in a non-portable solution. Therefore, in this work the authors propose a contactless system with IoT capabilities for the measurement of passive RF sensors. The sensor is inspired by a previous design [8], but it has been tailored to characterize a small volume of liquid samples. Both the proposed reader and the sensor have integrated antennas. Thus, the system presented results in a small-form factor and low-cost solution, leading to a full-portable system. The two main objectives of this work are the precise characterization of small volumes of liquids and the size and cost reduction of the system. Both goals are obtained with the proposed approach. The present article shows the design, implementation, and measurement of a fully functional demonstrator for the proposed system.

2. CONTACTLESS SENSING SYSTEM DEFINITION

The general framework of the proposed sensing system is shown in Figure 1. It is based on two elements: a contactless passive RF sensor and an Internet of Things Reader (IoT-R). The IoT-R can interrogate the passive sensor within a short range (1 cm approximately). This scheme allows an easy replacement of the sensor in case of failure or damage. The sensor is based on a printed monopole antenna loaded with a couple of SRRs [8] and is used to characterize the dielectric permittivity of small volumes of different liquids under test (LUT) which are placed over the sensor. On the other hand, the IoT-R generates the radio frequency signal needed to interrogate the contactless sensor, receives the response, digitizes that signal, and sends the data to a remote device (e.g., laptop, smartphone or tablet) through the Internet.

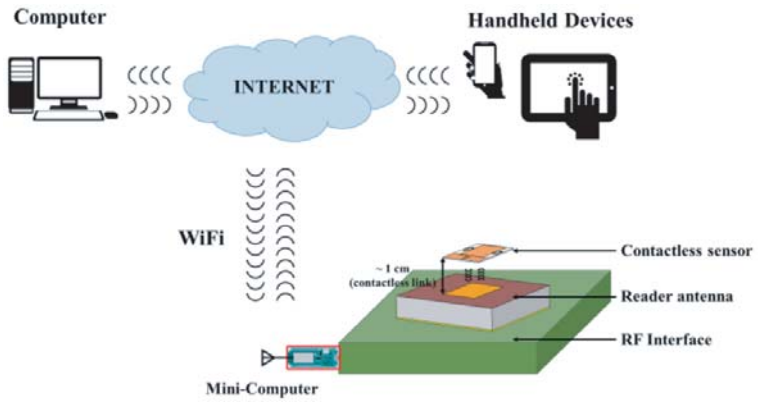

Figure 1. General framework of the proposed IoT sensing system.

The IoT-R follows the diagram shown in Figure 2. It is composed of four layers: radiating layer, RF interface, IoT mini-computer, and power unit. The RF interface generates a periodic frequency sweep needed to interrogate the sensor and detects the signal modified by the sensor. The radiating layer is based on a reader antenna which wirelessly transmits the signal generated by the RF interface and receives the RF signal modified by the sensor. This communication is made within a short range leading to a contactless system. The mini-computer digitizes the measurements and sends the data to the remote device. Finally, all the active elements of the previous layers are powered by the power unit, which is based on LM350AT commercial regulators by Texas Instruments.

The reader antenna is based on a patch antenna fed through capacitive coupling [17] in order to achieve the bandwidth for the proposed application. Hence, a contactless link is established between

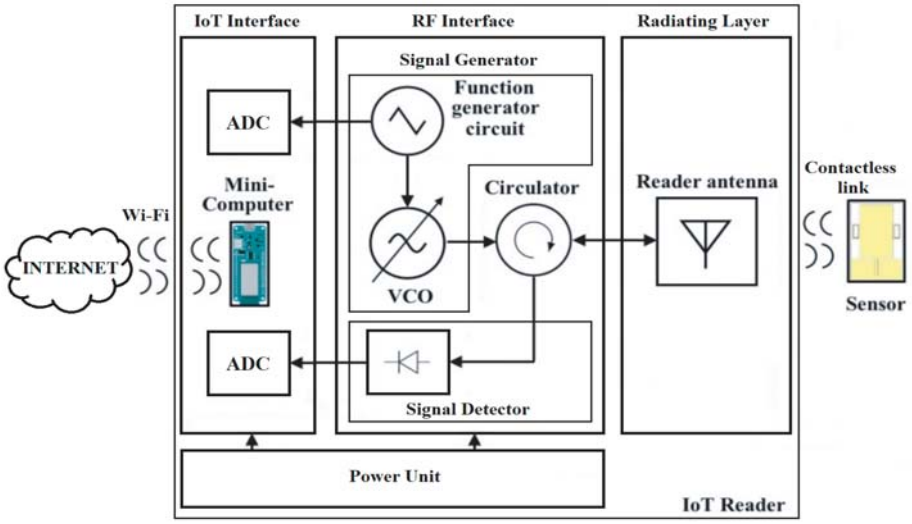

Figure 2. Layer diagram and components of the IoT contactless system.

the reader antenna and contactless sensor. The reader antenna, which is connected to the RF interface, interrogates the sensor. The signal sent from the reader antenna to the contactless sensor is modified by the sensor before being backscattered to the reader antenna. This modification depends on the LUT. Then, the backscattered signal is detected by RF interface, digitized and sent to a client by the mini-computer.

The RF interface is divided into two different blocks: a signal generator and a signal detector. The signal generator circuit performs the frequency sweep needed to interrogate the sensor. The signal generator circuit keeps the structure proposed in [16]. This signal generator is based on the Exar Corporation XR-2206 monolithic function generator integrated circuit and the Mini-Circuits JTOS-2000 VCO. However, the signal detector has been adapted to the new sensing system. Hence, the signal detector is formed by a Schottky diode detector (SDD), which provides an output voltage proportional to the input RF power, and a signal conditioning circuit based on an operational amplifier to optimize the digitalization of the signal. The SDD makes use of the HSMS-2850 Schottky diode by Broadcom, and the conditioning circuit is based on the Texas Instruments LM324N integrated circuit. As explained before, the generated and received signals are radiated by the reader antenna. These two signals are split by the circulator (model DPVCC64A by DPV CO company) which interconnects the reader antenna and the signal generator and detector. Finally, a mini-computer (Arduino MKR1000 [18]) digitizes the output signal of the SDD and sends the data wirelessly to a client.

The layout of the passive RF sensor is shown in Figure 3. This represents a single-layer printed monopole antenna loaded with a couple of SRRs. The SRRs introduce a maximum in the power backscatter by the monopole. The monopole is ended by a short-circuited coplanar waveguide (CPW) in order to optimize the power reflected to the reader. Thus, the sensing principle is based on the detection of this maximum when LUTs with different dielectric constants are placed over the sensor. When a LUT is situated over the structure, the effective permittivity increases while the frequency of the maximum in the backscatter decreases. The higher the dielectric permittivity of the LUT is, the lower the backscattered frequency is. The initial design of the sensor was done by using the equivalent circuit model approach presented in [8]. After that, CST Microwave Studio full-wave simulations were run in order to optimize the frequency range and sensitivity for the target application. The final dimensions of the sensor were $l_{\text{mon}} = 52\,\text{mm}$, $w_{\text{mon}} = 30.16\,\text{mm}$, $l_{\text{gnd}} = 20\,\text{mm}$, $w_{\text{gnd}} = 57.82\,\text{mm}$, $w_{\text{f}} = 3\,\text{mm}$, $g_1 = 0.5\,\text{mm}$, $g_2 = 0.33\,\text{mm}$, $g_3 = 0.33\,\text{mm}$, $g_4 = 0.3\,\text{mm}$, $g_5 = 1\,\text{mm}$, $w_{\text{lin}} = 0.33\,\text{mm}$, $l_{\text{SRR}} = 12.27\,\text{mm}$ and $w_{\text{SRR}} = 5.48\,\text{mm}$. The sensor was etched on a low-cost FR-4 substrate ($\varepsilon_{\text{r}} = 4$ and $\tan(\delta) = 0.015$) with 1.35-mm thickness and 17-µm copper metallization.

Figure 3 insets show the procedure to tailor the sensor for the measurement of liquid drops. The sensor was protected with a 1-mm thin film of adhesive Kapton ($\varepsilon_{\text{r}} = 3.5$ and $\tan(\delta) = 0.002$) in order

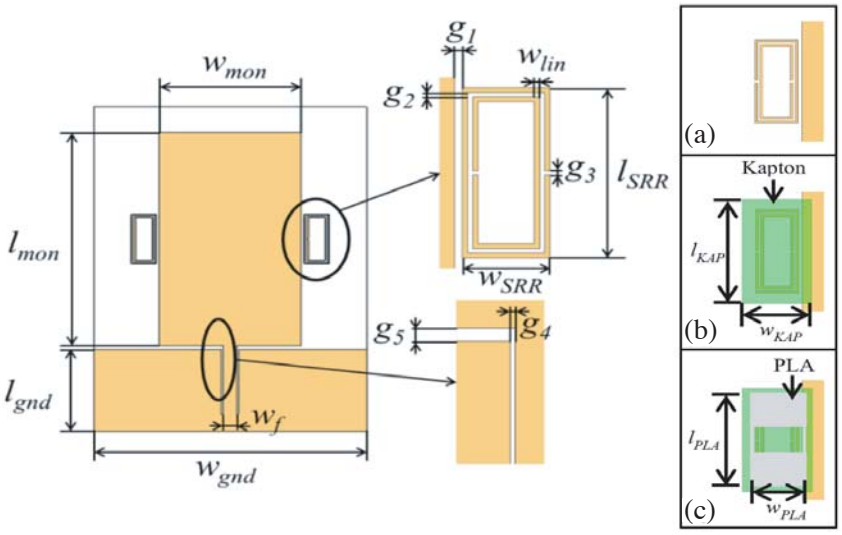

Figure 3. Layout of the contactless sensor. The Sensor is tailored to measure liquid drops: (a) SRR without protection, (b) SRR with a 1-mm thin film adhesive Kapton protection and (c) SRR with a 1-mm thin film adhesive Kapton protection and a PLA liquid holder.

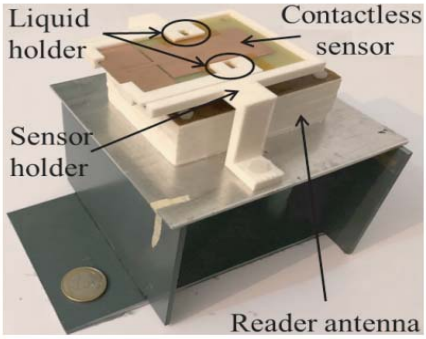

Figure 4. Manufactured reader antenna and contactless sensor.

to avoid the infiltration of the LUTs inside the substrate (Figure 3(b)), where $l_{\mathrm{KAP}} = 17\,\mathrm{mm}$ and $w_{\mathrm{KAP}} = 9.5\,\mathrm{mm}$. In addition, the SRRs have been covered with a coating layer manufactured with polylactic acid (PLA) [19, 20] by using a fused deposition modelling (FDM) 3D printer (Figure 3(c)), where $l_{\mathrm{PLA}} = 15\,\mathrm{mm}$ and $w_{\mathrm{PLA}} = 7.5\,\mathrm{mm}$. This structure leaves two gaps, one over each SRR, allowing the deposition of small volumes of LUT sample. Thus, with this liquid holder, the passive sensor can be used as a liquid sensor. Moreover, this novel approach only needs 4 ml approximately instead of over 250 ml needed in previous works [16], which allows the measurement of small volumes. In order to ensure the same measurement conditions for all the tests, a PLA sensor holder was manufactured with the FDM 3D printer. A picture of the final setup is shown in Figure 4.

3. RESULTS

Figure 5 shows the experimental setup of the whole sensing system. In this picture, all the system elements are included. The system is connected through the Internet to a remote client. The client was run on the laptop shown in the picture. In order to test the validity of the sensing system for the proposed application, multiple LUTs with different dielectric constants were measured. The whole set of liquids, their properties, and the measurements of the whole system are summarized in Table 1. As commented

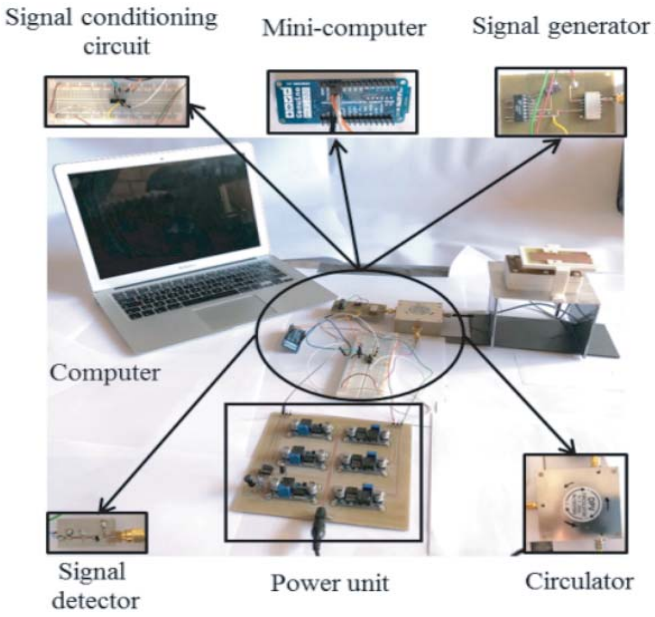

Figure 5. Demonstrator which contains all the system elements.

Table 1. List of the materials and results obtained with the whole sensing system.

Sample	Relative Permittivity (ε_r)	Δt [ms]
Free Space	1.00	1.32
Paraffin Oil	2.45	2.07
Olive Oil	2.94	2.16
Peanut Oil	2.94	2.17
Lemon Oil	3.03	2.17
Castor Oil	3.37	2.21
$CHCl_3$	5.77	2.41

before, the main application of this work is the dielectric characterization of oils, which is crucial for chemical and food industries. For this reason, the majority of LUTs are oils, whose permittivity is between 2 and 4. Moreover, the free space measurement is taken as reference. In addition, a LUT with higher permittivity (chloroform) is used to check the higher limit of the system. The different LUTs were firstly measured by using the 85070E dielectric characterization probe kit by Agilent.

Figure 6 plots the measurements of the whole sensing system for the different LUT samples. The triangular signal is proportional to the control signal of the VCO. In particular, two frequency sweeps are performed per period: the first one from 1.6 to 1.9 GHz (increasing sweep) and the second one from 1.9 to 1.6 GHz (decreasing sweep). In each sweep, a maximum voltage appears at a different time for each measurement (t_1 in the increasing sweep and t_2 in the decreasing sweep). As commented before, the maximums are related to the resonance of the SRRs introduced within the bandwidth of the monopole. Then, the detection principle is based on the time difference between these two maximums (t_2 and t_1, $\Delta t = t_2 - t_1$). Table 1 shows the time difference for each LUT. The same trend was measured for all the samples: the higher the time difference is, the higher the dielectric constant of the LUT is. These results are consistent with the original hypothesis. This dependency is shown in Figure 7. The time difference varies between 1.32 ms and 2.17 ms for dielectric permittivities between 1 and 5.77.

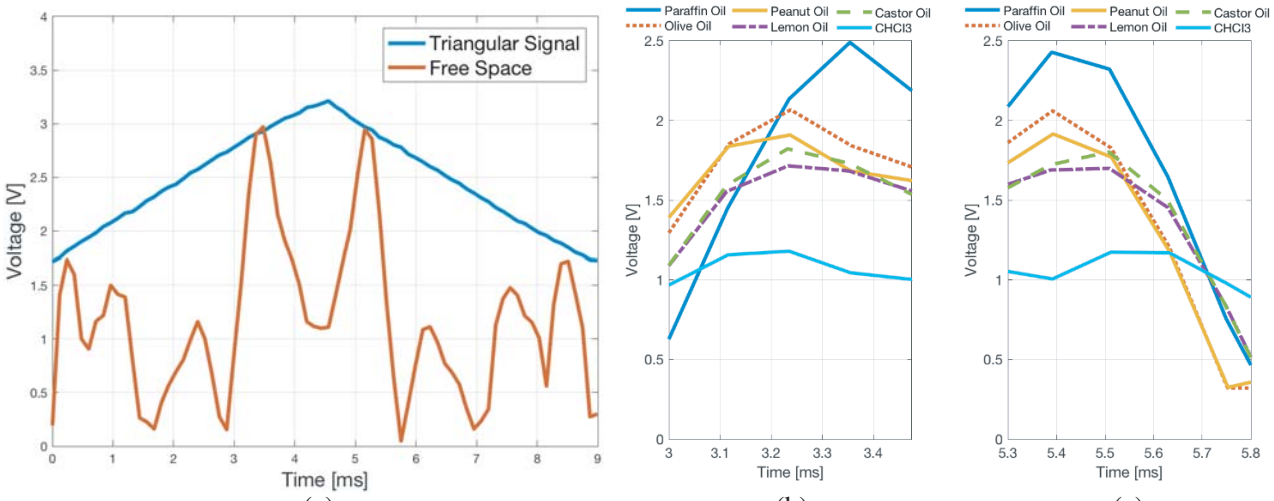

Figure 6. Measurements of the whole system: (a) Sweep signal and free space measurement, (b) maximums of the increasing sweep of all the measured samples and (c) maximums of the decreasing sweep of all the measured samples.

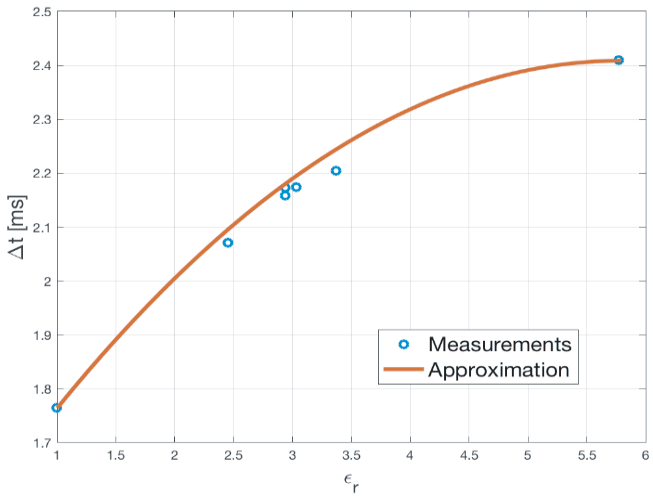

Figure 7. Measured time difference (Δt) (blue dots) and the approximation (solid red) for different LUTs.

Finally, an approximation to easily estimate the relative permittivity of the LUTs placed in the liquid holder by just measuring the time difference between the maximums is proposed:

$$\varepsilon_{\mathrm{r}} = 5.7896 - 9.2551\sqrt{1 - 0.4152 \cdot \Delta t\,[\mathrm{ms}]} \tag{1}$$

This expression was approximated considering all the experimental results in Table 1, and it is plotted in Figure 7 (solid, red). The resulting mean error between the measurements and the approximation is 0.27%.

4. CONCLUSIONS

In this work, a novel IoT contactless system for the dielectric characterization of small volumes of liquids is proposed. This system is composed of a passive sensor and an IoT-R. The sensor was covered with a Kapton protective layer and a PLA holder to measure liquid drops. The IoT-R letter represents a

great improvement with respect to previous works. On the one hand, the IoT-R proposed in [16] was a wireless solution but with a high form factor ($25 \times 45\,\text{cm}^2$), high weight (over 5 kg), and a complex setup (four external antennas which were pointed for each measurement). Moreover, the volume of liquid used was 250 ml approximately, which might be excessive for some applications. On the other hand, in this work the form factor is considerably reduced ($15 \times 15\,\text{cm}^2$) as well as the weight (below 1 kg), and there is no need of pointing the reader antenna to the contactless sensor, which simplifies the measurement procedure. A sensor holder was manufactured to always ensure the same position and, hence, achieve more reliable measurements. In this proposal, only 4 ml of liquid are needed, which represents a reduction of 98.4% with respect to previous works. Finally, a demonstrator of the whole sensing system was tested. This demonstrator was wirelessly connected to a remote client through the Internet, and a set of measurements were recorded in the client to check the correct performance of the system. These measurements show that the system can be used to estimate the permittivity of small volumes of liquids. An approximation of this estimation is proposed, which represents a small error (0.27%) with respect to the experimental results. These results confirm that the approach presented is a good solution as a contactless sensing system for the IoT.

REFERENCES

1. Da Fonseca, N. S. S. M., R. C. S. Freire, A. Batista, G. Fontgalland, and S. Tedjini, "A passive capacitive soil moisture and environment temperature UHF RFID based sensor for low cost agricultural applications," *2017 SBMO/IEEE MTT-S International Microwave and Optoelectronics Conference (IMOC)*, 1–4, Aguas de Lindoia, 2017.
2. Caccami, M. C., M. Y. S. Mulla, and G. Marrocco, "Wireless monitoring of breath by means of a graphene oxide-based radiofrequency identification wearable sensor," *2017 11th European Conference on Antennas and Propagation (EUCAP)*, 3394–3396, 2017.
3. Mason, A., O. Korostynska, J. Louis, L. E. Cordova-Lopez, B. Abdullah, J. Greene, R. Connell, and J. Hopkins, "Non-invasive in-situ measurement of blood lactate using microwave sensors," *IEEE Transactions on Biomedical Engineering*, Vol. 65, No. 3, 698–705, 2017.
4. Zhao, A., J. Zhang, and Y. G. Tian, "Miniaturization of UHD RFID tag antenna sensors for corrosion characterization," *IEEE Sensors Journal*, Vol. 17, No. 23, 7908–7916, 2017.
5. Suwalak, R., C. Phongcharoenpanich, D. Torrungrueng, and M. Krairiksh, "Determination of dielectric property of construction material products using a novel RFID sensor," *Progress In Electromagnetics Research*, Vol. 130, 601–617, 2012.
6. Jalo, J., H. P. Sillanpaa, and R. M. Makinen, "Radio interface design for inkjet-printed biosensor applications," *Progress In Electromagnetics Research*, Vol. 142, 409–422, 2013.
7. Galindo-Romera, G., F. J. Herraiz-Martínez, M. Gil, J. J. Martínez-Martínez, and D. Segovia-Vargas, "Submersible printed split-ring resonator-based sensor for thin-film detection and permittivity characterization," *IEEE Sensors Journal*, Vol. 16, No. 10, 3587–3596, 2016.
8. Carnerero-Cano, J., G. Galindo-Romera, J. J. Martínez-Martínez, and F. J. Herraiz-Martínez, "A contactless dielectric constant sensing system based on a split-ring resonator-loaded monopole," *IEEE Sensors Journal*, Vol. 18, No. 11, 4491–4502, 2018.
9. Sinha, M., V. Killamsetty, B. Mukherjee, "Near field analysis of rdra loaded with split ring resonators superstrate," *Microwave and Optical Technology Letters*, Vol. 60, No. 2, 472–478, Wiley, 2018.
10. Mukherjee, B., P. Patel, and J. Mukherjee, "A novel hemispherical dielectric resonator antenna with complementary split-ring-shaped slots and resonator for wideband and low cross-polar applications," *IEEE Antennas and Propagation Magazine*, Vol. 57, No. 1, 120–128, Feb. 2015, doi: 10.1109/MAP.2015.2397113.
11. Laxman Kumar, A., A. Ranjan, M. Chauhan, V. K. Killamsetty, and B. Mukherjee, "Circular SRR shaped UWB antenna with WiMAX band notch characteristics," *2018 IEEE Radio and Antenna Days of the Indian Ocean (RADIO)*, 1–2, Grand Port, 2018, doi: 10.23919/RADIO.2018.8572343.

12. Juan, C. G., E. Bronchalo, B. Potelon, C. Quendo, E. Ávila-Navarro, and J. M. Sabater-Navarro, "Concentration measurement of microliter-volume water-glucose solutions using Q factor of microwave sensors," *IEEE Transactions on Instrumentation and Measurement*, Vol. 68, 2621–2634, Jul. 2019.
13. Sharafadinzadeh, N., M. Abdolrazzaghi, and M. Daneshmand, "Highly sensitive microwave split ring resonator sensor using gap extension for glucose sensing," *2017 IEEE MTT-S International Microwave Workshop Series on Advanced Materials and Processes for RF and THz Applications, IMWS-AMP 2017*, Vol. 2018, 1–3, Institute of Electrical and Electronics Engineers Inc., Jan. 2018.
14. Tiwari, N. K., S. P. Singh, and M. J. Akhtar, "Quad band metamaterial inspired planar sensor for dispersive material testing," *IEEE MTT-S International Microwave and RF Conference, IMaRC 2017*, 120–123, Institute of Electrical and Electronics Engineers Inc., Aug. 2018.
15. Altintaş, O., M. Aksoy, E. Ünal, and M. Karaaslan, "Chemical liquid and transformer oil condition sensor based on metamaterial-inspired labyrinth resonator," *Journal of the Electrochemical Society*, Vol. 166, No. 6, B482–B488, 2019.
16. Galindo-Romera, G., J. Carnerero-Cano, J. J. Martínez-Martínez, and F. J. Herraiz-Martínez, "An IoT reader for wireless passive electromagnetic sensors," *Sensors*, Vol. 17, No. 4, 693, 2017.
17. Hazdra, P., M. Mazánek, and J. Cermák, "Wideband rectangular microstrip patch antenna using L-probe feeding system," *Radioengineering*, Vol. 16, 37–41, 2007.
18. Arduino MKR1000, Available online: https://www.arduino.cc/en/Main/ArduinoMKR1000, accesed on Jun. 06, 2019.
19. Dichtl, C., P. Sippel, and S. Krohns, "Dielectric properties of 3D printed polylatic acid," *Advances in Materials Science and Engineering*, Hindawi, ed., Vol. 2017, Article ID 6913835, 10 pages, 2017, doi:10.1155/2017/6913835.
20. Felício, J. M., C. A. Fernandes, and J. R. Costa, "Complex permittivity and anisotropy measurement of 3D-printed PLA at microwaves and millimeter-waves," *2016 22nd International Conference on Applied Electromagnetics and Communications (ICECOM)*, 1–6, Dubrovnik, 2016, doi: 10.1109/ICECom.2016.7843900.